Title

Effects of sulfate and magnesium on cement degradation under geologic CO2 sequestration conditions

Authors

Guo, Jilong
Cao, Bo
Steefel, Carl I
et al.

Publication Date

2017-08-01

DOI

10.1016/j.ijggc.2017.04.017

Peer reviewed

Effects of sulfate and magnesium on cement degradation under geologic CO_2sequestration conditions

Author links open overlay panelJilongGuo[ab]BoCao[b]Carl I.Steefel[c]JiaweiChen[a]YandiHu[b]
Show more

https://doi.org/10.1016/j.ijggc.2017.04.017Get rights and content

Highlights

- Effects of sulfate and magnesium on cement degradation were investigated under GCS conditions.
- First time observation of gypsum formation on cement reacted under relevant GCS condition.
- The formation of gypsum was due to low solution pH and a low liquid-to-solid ratio.
- Gypsum coating on cement surface can protect cement from further CO_2 attack.

Abstract

For safer geologic CO_2 sequestration (GCS), it is important to understand CO_2-brine-cement interactions, which affect wellbore integrity. However, potential effects of sulfate and magnesium ions on cement degradation under GCS conditions are not well understood. Here Class H Portland cement were reacted in brines containing 0.05 M sulfate and/or magnesium ions under both GCS (50 °C and 100 atm CO_2) and control (50 °C and atmospheric pressure) conditions. Using optical microscopy and scanning electron microscope coupled with energy dispersive spectrometry and electron back scattered electron (SEM-EDS/BSE), slower cement carbonation rates were observed in the presence of sulfate under GCS conditions, because of gypsum precipitation on cement surfaces. Calcite rather than gypsum formed in both the inner layers of cement samples reacted under GCS conditions, and on cement surfaces reacted under atmospheric pressure conditions. Under GCS conditions, the dissolved CO_2 lowered the pH of the solution surrounding cement surfaces, thus favoring the formation of gypsum over calcite on cement surfaces; while the high pH condition in pore solution inside cement favors the formation of calcite over gypsum. The presence of magnesium had

no significant effect on cement degradation under GCS conditions, as brucite, magnesium carbonates and magnesium calcite did not form, due to the low pH at cement surface and the limited diffusion of Mg into cement inner layers.

- **Previous** article
- **Next** article

Keywords

Geologic CO_2 sequestration (GCS)
Cement degradation
Sulfate
Magnesium
Gypsum
Calcite

1. Introduction

Geologic CO_2 sequestration (GCS) is considered as a feasible strategy to reduce anthropologic CO_2 emissions (IPCC, 2005). For CO_2 injection wells, Class H Portland cement is often used as sealing materials during well construction and after CO_2 injection. However, the injected CO_2 can dissolve in brine, lowering its pH and increasing its dissolved inorganic carbon concentrations. The acidic brine can react with cement, causing cement degradation and potential CO_2 leakage (Carey, 2013, Zhang and Bachu, 2011, Carey et al., 2007, Crow et al., 2010, Scherer et al., 2011). Therefore, for safer and more effective GCS operations, a better understanding of CO_2-brine-cement interactions under relevant GCS conditions is needed.

In recent years, such interactions have been studied under relevant GCS conditions, and the effects of fly ash addition (Kutchko et al., 2009) and cement-curing conditions (Kutchko et al., 2007, Kutchko et al., 2008) on cement degradation were studied. Such interactions were also studied in the scenarios of H_2S-cojection (Jacquemet et al., 2008, Hawthorne et al., 2011, Kutchko et al., 2011, Jacquemet et al., 2012, Zhang et al., 2013, Zhang et al., 2014) with varied flow/diffusion conditions of formation water (Duguid, 2009, Duguid and Scherer, 2010). In these studies, sodium chloridewas added in deionized water to represent the salt compositions of formation brines (Carey, 2013, Zhang and Bachu, 2011). However, in deep saline aquifers at GCS sites, the brines usually also contain high concentrations of sulfate and magnesium ions ranging over 0.01–0.05 M and 0.02–0.24 M,respectively (De Silva et al., 2015, Keller, 1983). In addition, sulfate ions could also form during H_2S co-injecting with CO_2 (Kutchko et al.,

2011). The presence of high concentrations of sulfate and magnesium ions in brines may affect cement degradation under GCS conditions greatly. For example, a core sample from a 19-year-old well prior to CO_2injection was reported to have experienced sulfate attack, with ettringite formation and elevated porosity (Scherer et al., 2011). Therefore, it is important to understand the effects of sulfate and magnesium ions on cement degradation under relevant GCS conditions.

Under ambient conditions, cement degradation in the presence of sulfate and magnesium ions has been investigated for decades. For sulfate ions, their effects on cement degradation have been reported to be related to the coexisting cations (Ca^{2+}, Na^{+}, or Mg^{2+}) (Neville, 2004, Pabalan et al., 2009). Specifically, Ca^{2+} and SO_4^{2-} can react with C_3A and form ettringite, which will cause expansion and cracking (Neville, 2004). Na^{+} and SO_4^{2-} can react with C—H and form gypsum, although the roles of gypsum formation on further cement degradation are still controversial. In Tian and Cohen's studies, the formation of gypsum led to cement expansion and accelerated degradation (Tian and Cohen, 2000a, Tian and Cohen, 2000b, Santhanam et al., 2003). In some other studies, in contrast, no cement expansion was observed (Neville, 2004, Santhanam et al., 2003). In the presence of Mg^{2+}, brucite could form accelerating Ca^{2+}release and gypsum precipitation (Santhanam et al., 2003), which can result in even more severe cement degradation (Neville, 2004).

These previous studies showed the significant effects of sulfate and magnesium ions on cement degradation under ambient conditions. However, their effects on cement degradation under relevant GCS conditions (i.e., under high temperature and high CO_2 pressure in brines with high salinity) are not well understood. To our knowledge, only recently, Li et al., 2015a, Li et al., 2015b reported the effects of sulfate ions on newly hardened cement under 95 °C and ~100 atm CO_2 condition. In their study, Li et al., 2015a, Li et al., 2015b proposed that the presence of sulfate could protect cement from CO_2 attack through sulfate adsorption and/or coating of gypsum on calcite ($CaCO_3$) grains in carbonated layer. However, gypsum was not directly detected in their experiments. Therefore, the question remains whether gypsum could form in the presence of sulfate under GCS conditions, a process which could have important implications for the assessment of cement integrity. Moreover, the effects of Mg^{2+} on cement degradation under GCS conditions were not reported.

This study aimed to understand the effects of sulfate and magnesium ions on cement degradation under relevant GCS conditions. Class H Portland cement was reacted in brines with/without SO_4^{2-} and/or Mg^{2+}. After reaction, the layered structures as well as the chemical and mineralogical compositions of reacted cement samples were analyzed

by scanning electron microscopy (SEM) coupled with energy dispersive spectrometry (EDS) and back scattered electron (BSE) and X-ray diffraction (XRD). Gypsum and calcite were detected on the surface layer and inner layers of cement samples reacted in SO_4^{2-}-containing brines, respectively. The controlling mechanisms for gypsum and calcite formation at GCS conditions were elucidated. Different carbonation depths of reacted cements in brines with/without $SO_4^{2-}$and/or Mg^{2+} were also measured, and these were used to determine cement degradation rates.

2. Materials and methods

2.1. Synthetic brine preparation

To study the effects of aqueous Mg^{2+} and SO_4^{2-} ions on cement degradation under GCS conditions, four synthetic brines were prepared: A: NaCl; B: NaCl + $MgCl_2$; C: NaCl + Na_2SO_4; and D: NaCl + $MgSO_4$ (Table 1). For all solutions, the ionic strength (IS = 0.65–0.67 M, Table 1) and initial pH values (3.00–3.21, Table 1) at 50 °C under 100 atm were similar, as calculated using Geochemist's Workbench (GWB student, Release 11, RockWare, Inc.). The details of solution calculations under relevant GCS conditions can be found in our previous publications (Hu et al., 2011, Garcia et al., 2012, Hu and Jun, 2012, Hu et al., 2013).

Table 1. Synthetic brine compositions for cement degradation experiments.

Solutions	Na^+ (mM)	Cl^- (mM)	Mg^{2+} (mM)	SO_4^{2-} (mM)	Ionic Strength[a](IS, M)	pH[a]
A (NaCl)	625	625	0	0	0.67	3.02
B (NaCl + Mg^{2+})	490	590	50	0	0.65	3.00
C (NaCl + SO_4^{2-})	610	510	0	50	0.65	3.21
D (NaCl+Mg^{2+} + SO_4^{2-})	500	500	50	50	0.65	3.18

Note:

a Ionic strength and pH values are calculated using GWB under 100 atm CO_2 at 50 °C.

2.2. Cement casting, curing and degradation

Class H Portland cement offered by Leigh Company (Houston, TX) was used to prepare cement slurry samples with a water-to-cement (w/c) ratio of 0.38, according to

American Petroleum Institute (API) recommended practice (API, 2005). The slurry was cast in cylinder molds with dimensions of 0.5 cm (d) × 2.0 cm (h), and cured at 50 °C under 100 atm N_2 pressure, representing reservoir conditions before CO_2 injection. After the first 3 days of curing, the hardened cement samples were demolded, submerged in different synthetic brines (solutions A, B, C, or D in Table 1), and continuously cured at 50 °C under 100 atm N_2 for another 25 days, to achieve further chemical and structural development. Curing experiments were conducted in a high-pressure reactor (Parr Instrument Company, IL) connected to a high-pressure syringe pump (Teledyne ISCO, Lincoln, NE). Temperature and pressure inside the reactor were controlled with the accuracy of ±1 °C and ±1 atm. Details of the high temperature and high pressure setup (high P/T) can be found in our previous publications (Hu et al., 2011, Garcia et al., 2012, Hu and Jun, 2012, Hu et al., 2013).

After curing for a total of 28 days, the cement samples were transferred to clean polypropylene (PP) tube, and submerged in freshly prepared synthetic brines (A, B, C, or D in Table 1), with the same salt compositions as the curing experiments and a liquid-to-solid volume ratio of 10:1. Then, the tubes were placed in the high P/T setup at 50 °C under 100 atm of CO_2, and cement degradation under this relevant GCS conditions were conducted for 3, 7, 14, or 28 days.

To understand the effects of CO_2 injection on cement degradation, cement curing and degradation experiments were also conducted in synthetic brines following the same procedures at 50 °C, but under atmospheric pressure (1 atm air).

2.3. Characterization of reacted brines and cement samples

After cement degradation for 3, 7, 14, or 28 days, CO_2 was slowly released from the reactor, and the reacted cement samples were taken out. The reacted brines were filtered (0.22 μm Nylon) and acidified by 2% nitric acid and the dissolved Ca concentrations were measured by atomic absorption spectrometer (AAS, AAnalyst 200, PerkinElmer). Based on the measured Ca concentration and the aqueous sulfate and carbonate concentrations, the solutions' saturation indices (SI) with respect to calcite and gypsumwere calculated using Geochemist's Workbench (GWB student, Release 11, RockWare, Inc.).

In previous studies of cement degradation under relevant GCS conditions, layered structures were observed to have formed in the reacted cement samples (Kutchko et al., 2007, Kutchko et al., 2008, Kutchko et al., 2009, Duguid, 2009, Duguid and Scherer, 2010, Jacquemet et al., 2012, Carey, 2013, Li et al., 2015a, Li et al., 2015b). To identify the layered structures, reacted cement samples were rinsed by ultrapure water, dried in

air, cut into small cylinders by diamond saw and polished with sandpapers. Then, both optical microscopy(Optem, Qioptiq) and scanning electron microscopy (SEM, Zeiss Merlin Compact) were utilized to observe the layered structures of the reacted cement samples. The elemental compositions and structures of reacted cement samples were characterized by SEM coupled with EDS and BSE. To identify the mineral compositions of reacted cement samples, under optical microscope, powder samples were scratched off from the reacted cement samples layer-by-layer with a blade until it reached the unreacted cement core. Then, the collected powder samples were grounded by mortar and pestles and then analyzed by X-ray diffraction (XRD, Miniflex 600, Rigaku). For control experiments conducted at 50 °C under 1 atm air, the outer layers of reacted cement samples were too thin to collect enough powders for XRD analyses. Therefore, solid precipitates in the reacted solution were collected instead, and were air dried for XRD measurements.

3. Results and discussion

3.1. Identification of layer structures of reacted cement samples

Cement samples reacted under relevant GCS condition (50 °C and 100 atm of CO_2) and atmospheric pressurecondition (50 °C and 1 atm of air) were examined using optical microscopy. For cement samples reacted in different brine solutions (Table 1) under atmospheric pressure, only a thin white layer was observed outside the cement rim (Fig. S1 in Supporting information), indicating slow cement degradation under these conditions. For all cement samples reacted under relevant GCS conditions in different brine solutions (Table 1), a four-layer structure was observed by both optical microscopy and SEM. Based on SEM-BSE observations together with EDS elemental mapping and XRD analysis, four layers were identified from rim to core as: (1) Layer I: white precipitation layer; (2) Layer II: yellow leached layer; (3) Layer III: black carbonated layer; and (4) Layer IV: grey unreacted cement core.

Samples reacted in the presence of sulfate with or without magnesium (Table 1, solution C: NaCl + Na_2SO_4; D: NaCl + $MgSO_4$) showed similar layered structures, and the layered structures after reaction in solution C were shown in Fig. 1, Fig. 2. Based on optical microscopy, the reacted cement samples were covered by a white layer (Layer I in Fig. 1). SEM-BSE images (Fig. 2) showed that the structures of Layer I were quite different from those of unreacted cement core (Layer IV), and large crystals between ~50–100 μm were observed in Layer I. EDS measurements of these crystals showed that their principal elements were Ca, O, and S (Fig. S2 in Supporting information). Elemental mapping of the entire Layer I (Fig. 3) showed that Si was rarely detected

anywhere, while enrichment of Ca and S correlated well with the large crystals, indicating that Layer I was primarily composed of calcium sulfate precipitates (Fig. 3). The white precipitates were easily scratched from the reacted cement surfaces, and XRD (Fig. 4) analysis confirmed that the principal mineral phase in Layer I was gypsum ($CaSO_4 \cdot 2H_2O$).

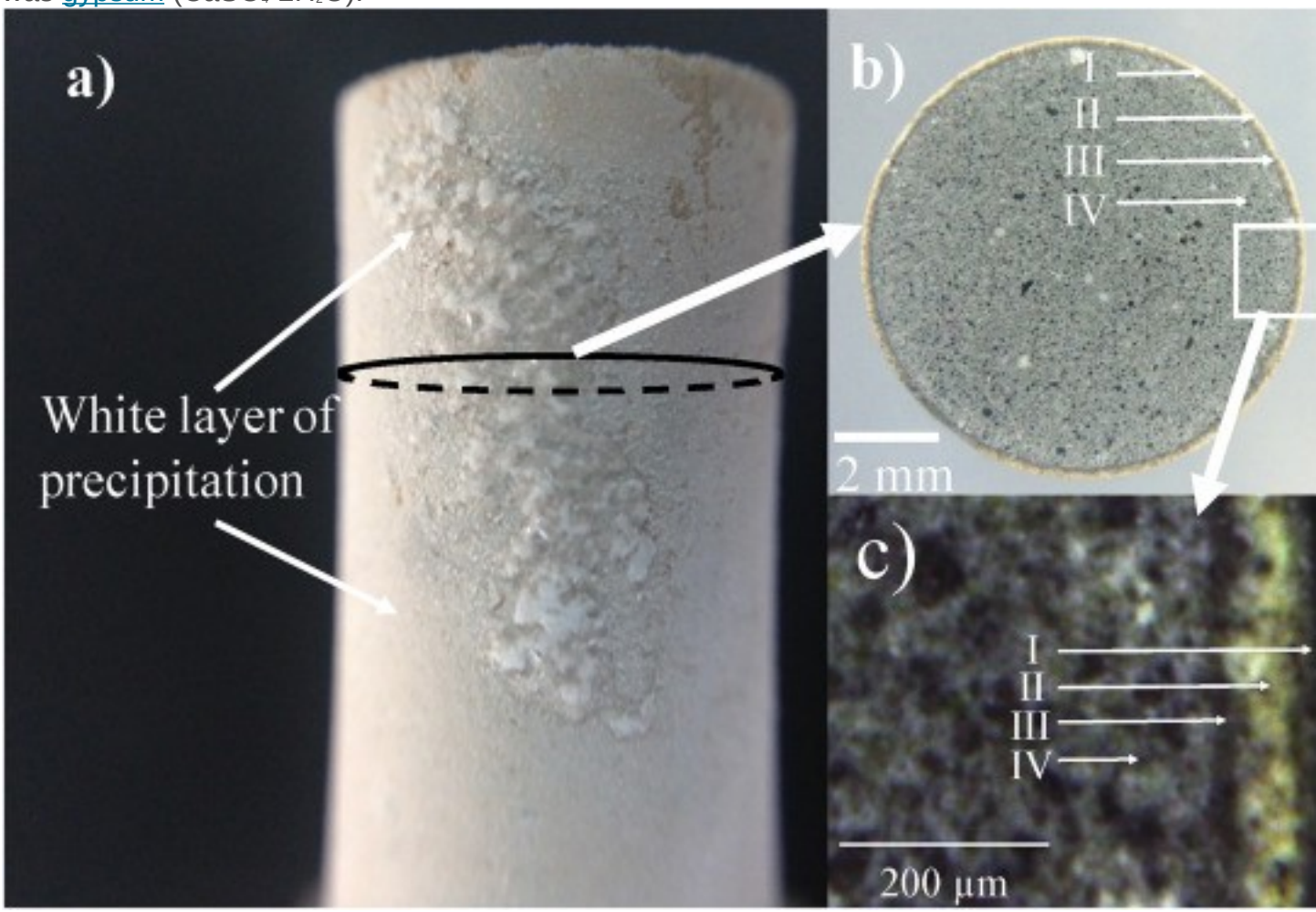

1. Download high-res image (835KB)
2. Download full-size image

Fig. 1. Optical microscopy images showing layered structures of cement samples reacted in the presence of sulfate (Solution C in Table 1) under relevant GCS conditions: I: White precipitation layer, II: Yellow leached layer, III: Black carbonated layer, IV: Grey unreacted cement core. (For interpretation of the references to color in this figure legend, the reader is referred to the web version of this article.)

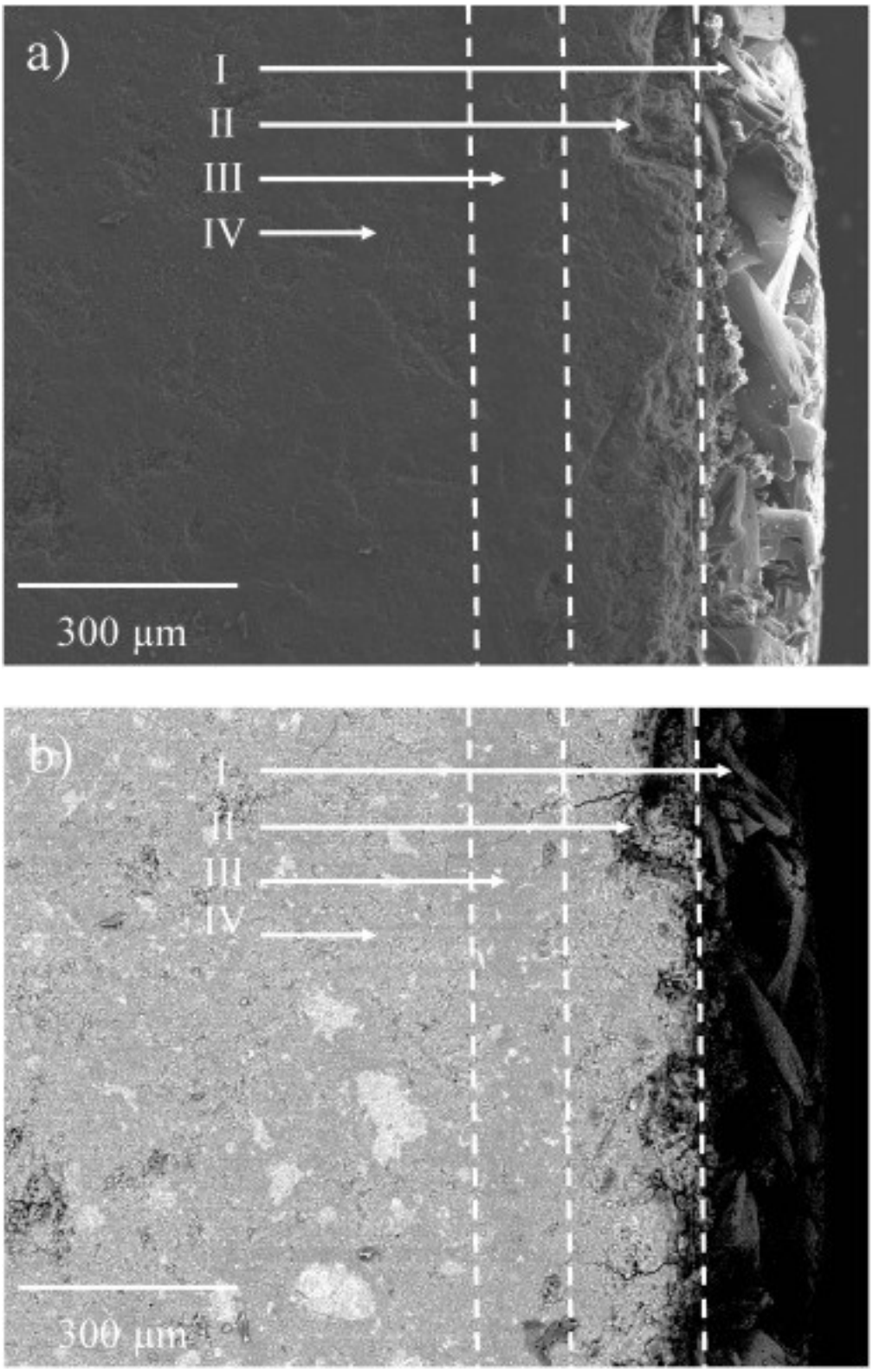

1. Download high-res image (1MB)
2. Download full-size image

Fig. 2. SEM (a)-BSE (b) images showing layered structures of cement reacted in the presence of sulfate (Table 1, solution C: NaCl + Na_2SO_4) under relevant GCS conditions (50 °C and 100 atm of CO_2): I: precipitation layer; II: leached layer; III: carbonated layer; and IV: unreacted cement core.

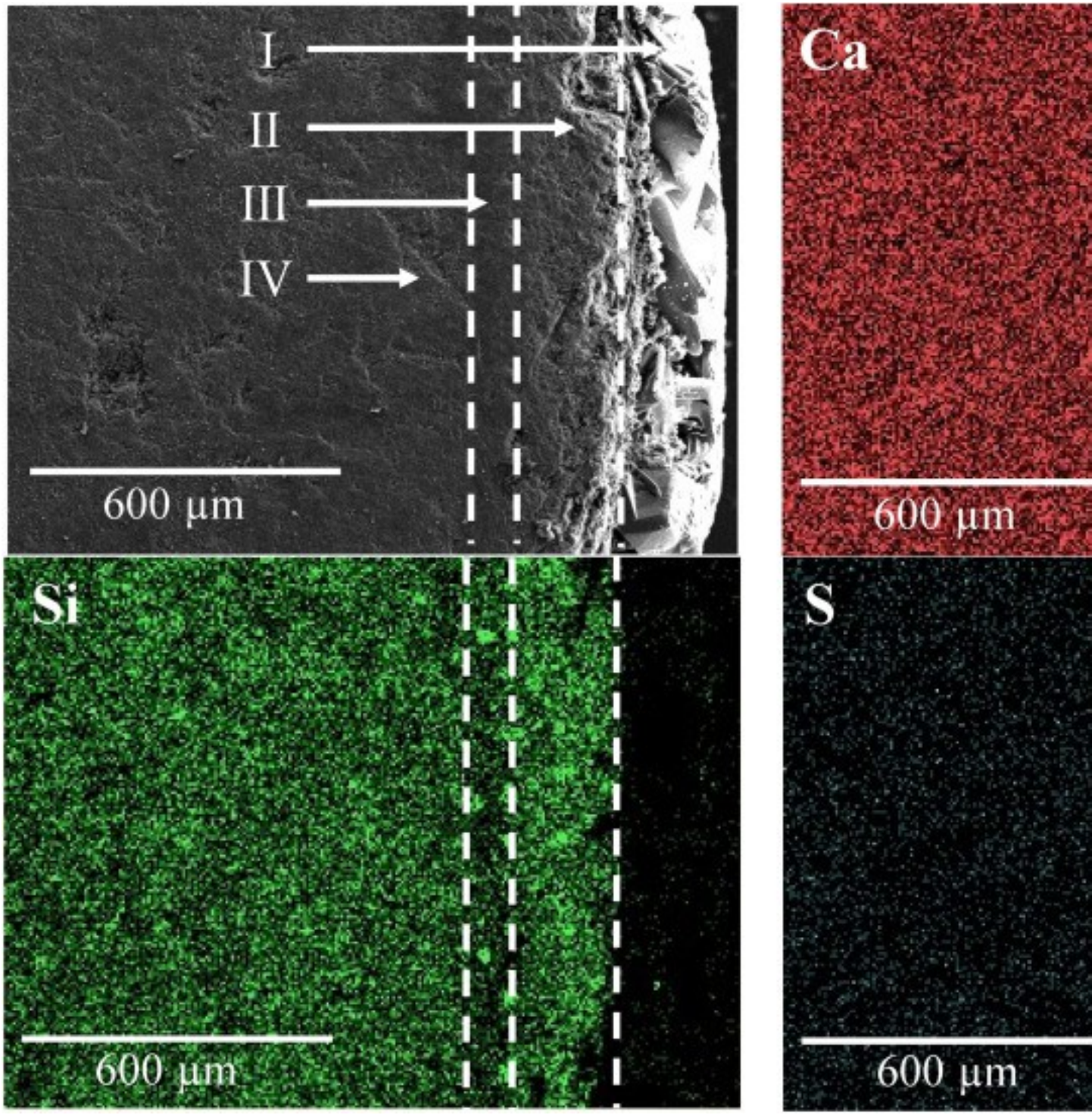

1. Download high-res image (3MB)

2. Download full-size image

Fig. 3. SEM-EDS mapping showing layered structures of cement reacted in the presence of sulfate (Table 1, solution C: NaCl + Na_2SO_4) under relevant GCS conditions (50 °C and 100 atm of CO_2): I: precipitation layer; II: leached layer; III: carbonated layer; and IV: unreacted cement core.

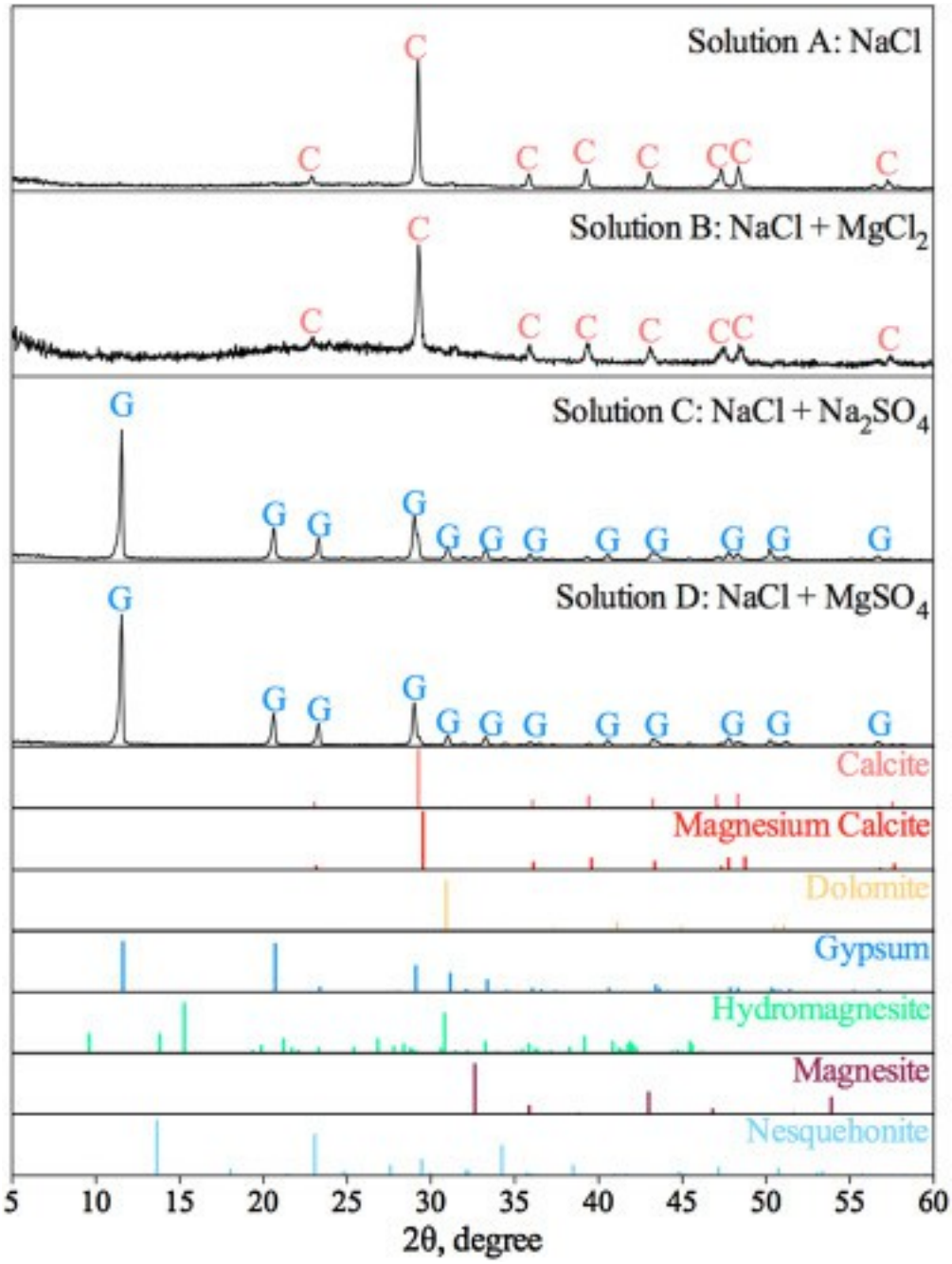

1. Download high-res image (436KB)
2. Download full-size image

Fig. 4. XRD analysis of Layer I (white precipitation layer) on surfaces of cement samples reacted in different brine solutions (Table 1, solution A–D) under relevant GCS conditions (50 °C and 100 atm of CO_2). Calcite (C) and gypsum (G) were the main mineral phase for cement samples reacted in the absence (solutions A and B) and presence (solutions C and D) of sulfate.

The yellow layer II (Fig. 1, Fig. 2) was identified as the leached region reported by Kutchko et al., 2007, Kutchko et al., 2008, Kutchko et al., 2009, Li et al., 2015a, Li et al., 2015b based on its Ca depletion and Si enrichment determined by EDS mapping (Fig. 3). The main reaction in the leached region was the dissolution of calcite by carbonic acid:

(1) $CaCO3+H2CO3 \rightarrow Ca2++2HCO3-$

This reaction was reported to result in a higher porosity and roughness as compared to the unreacted cement, which was observed here (Fig. 2). The yellow Layer II and the black Layer III were much denser than the white precipitation Layer I, and required more force to scratch powder off from these two layers. Also, Layer III was thin, making it difficult to well control the layer-by-layer scratching, therefore, powders were collected from these two layers together and were used for XRD analysis. Interestingly, calcite rather than gypsum was detected in Layer II and/or III as the principal mineral phase (Fig. 5), and small amounts of aragonite were detected in Layer II and/or III as well. Recently Li et al. (2015b) also observed a yellow layer and proposed that the color may correlate with Fe (III) absorption or Fe(III)-containing mineral precipitation. In Li et al.'s (2015b) and our current study, no crystallized Fe (III) (hydr)oxides were detected by XRD (Fig. 5), indicating that the Fe(III) species may not be well-crystallized or too sparse to be detected (Dai and Hu, 2015, Dai et al., 2016).

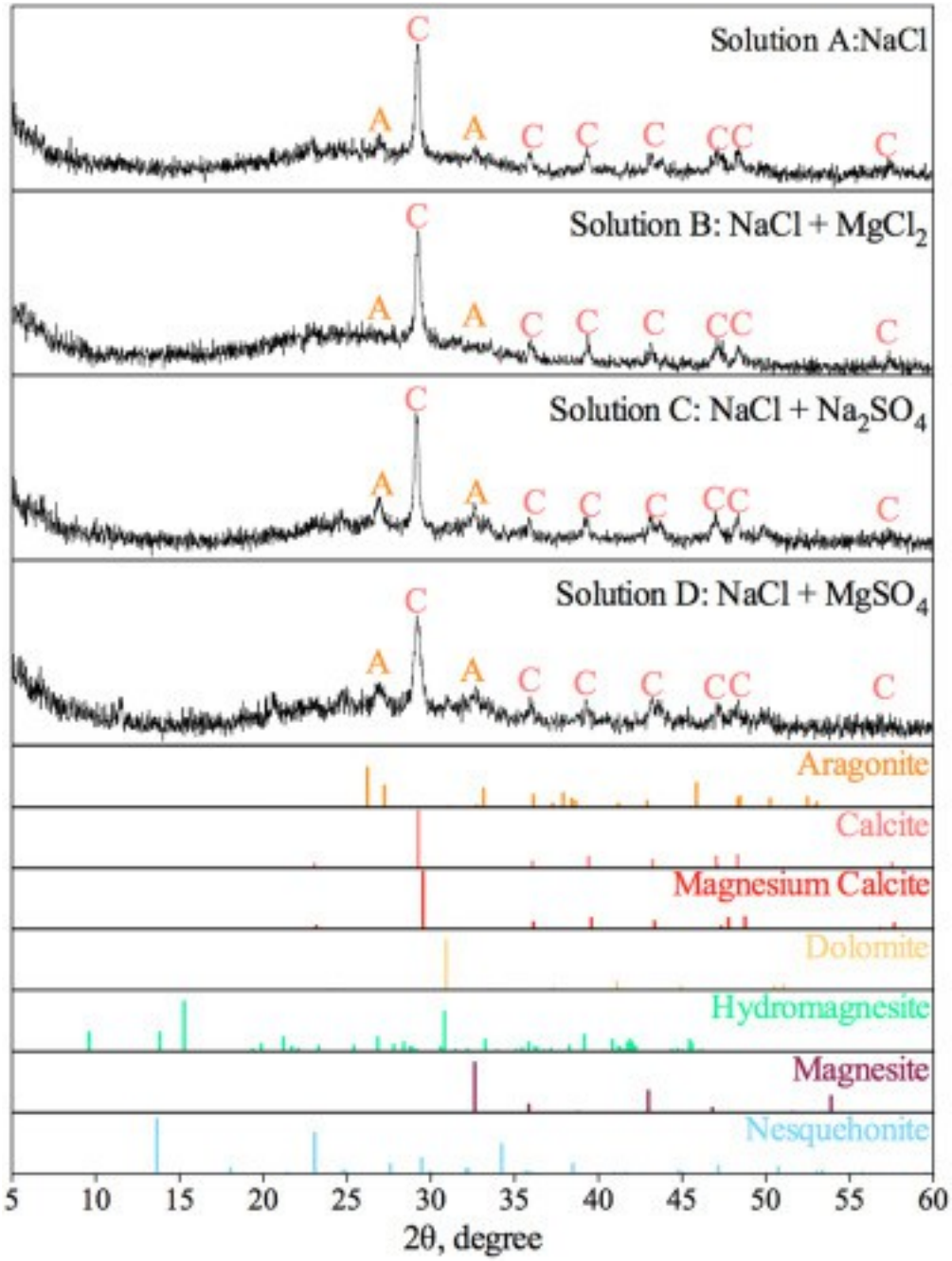

1. Download high-res image (473KB)
2. Download full-size image

Fig. 5. XRD analysis of powders scratched from Layer II (leached layer) and Layer III (carbonated layer) of cement samples reacted in different brine solutions (Table 1, solution A-D) under relevant GCS conditions (50 °C and 100 atm of CO_2). For cement samples reacted in all solutions, calcite (C) and small amounts of aragonite(A) were detected, and no gypsum (G) was detected.

The black Layer III (Fig. 1, Fig. 2) was identified as the carbonated region based on its low Si and high Ca composition (Fig. 3) and its lower porosity (Fig. 2) than the leached Layer II. With higher pH than Layer II, bicarbonateand/or carbonate was the dominant carbon species in Layer III as compared to carbonic acid. Therefore, the principal reaction in layer III was calcite precipitation as described by Eq. (2).

(2)$Ca2++OH-+HCO3- \rightarrow CaCO3+H2O$

For cement samples reacted in solution without sulfate (Table 1, solutions A and B) under relevant GCS condition, a similar four-layer structure was also observed (Fig. S4 in Supporting information). Based on both XRD (Fig. 4) and SEM-EDS (Fig. S2 in Supporting information) measurements, the precipitation Layer I was mainly composed of calcite, and calcite and small amounts of aragonite were detected in Layer II and/or III.

In summary, for all cement samples reacted under relevant GCS conditions, a four-layer structure was observed. Surface Layer I was consisted of gypsum precipitates where sulfate was present in the solution (solution C and D) and of calcite precipitates where sulfate was absent (solution A and B). In contrast, in the inner Layers II and III, calcite was detected as the main mineral phase after reaction in all solutions (A–D) with or without sulfate presence. The mechanisms for calcite and gypsum formation are discussed in the following Section 3.2.

3.2. Effects of pH on gypsum and calcite formation during cement degradation

As discussed in Section 3.1, under relevant GCS condition, in the absence of sulfate, calcite was the principal mineral phase in the surface precipitation layer (Figs. 2, S2 and S4 in Supporting information). Using Geochemist's Workbench (GWB), the saturation index (SI = Log({Ca^{2+}}{CO_3^{2-}}/K_{sp}), $K_{sp} = 10^{-8.88}$ at 50 °C) for calcite under 100 atm CO_2 pressure in solution A was calculated to be −2.13. Although the bulk solution was undersaturated with respect to calcite, with Ca^{2+} supply from the leached Layer II (Eq. (1)), Ca^{2+} ion concentrations in the local solution around Layer I were likely to be higher than in the bulk solution (Hu et al., 2011). As a result, calcite could precipitate in Layer I. It is also possible that calcite precipitation occurred when $CO_2$was released from the reactor, which would have resulted in a higher solution pH favoring calcite precipitation.

In the presence of sulfate, in the surface precipitation layer I (Figs. 2–4 and S2 in Supporting information), gypsum was the main mineral phase and no calcite was detected. Using GWB, the saturation indices (SIs) of bulk solution C with respect to gypsum ($K_{sp} = 10^{-4.52}$ at 50 °C) and calcite were calculated to be −0.68 and −2.17,

respectively. Although the bulk solution was undersaturated with respect to both mineral phases, the local concentration of Ca^{2+} surrounding the surface of cement was likely to have been higher than that in bulk solution (Hu et al., 2011), with local Ca^{2+} supply from Layer II (Eq. (1)). As the bulk solution was much closer to saturation with respect to gypsum (SI = −0.68) than calcite (SI = −2.17), the local solution around Layer I would have reached supersaturation with respect to gypsum while the solution was still undersaturated with respect to calcite. Therefore, gypsum precipitation was favored over calcite on cement surface Layer I. As the solubility of gypsum is not affected by either solution pH or aqueous inorganic carbonate concentration, gypsum precipitation was likely to have occurred during cement degradation under high P/T conditions rather than during CO_2 release at the end of the degradation experiments.

It is interesting to note that, for cement samples reacted in the presence of sulfate, calcite rather than gypsum was detected in the inner Layers II and III (Fig. 5). We hypothesize that this was caused by the concentration gradient of proton from bulk solution to the inner layers, i.e., the low pH in solutions near the cement surface favored gypsum formation, while the higher pH in pore solutions within the inner layers of cement favored calcite formation. As shown in Fig. 6: at cement surfaces, with low solution pH of 4.04 (calculated by GWB), the dominant carbon species was carbonic acid and the activity of carbonate ions ($\{CO_3^{2-}\} = 10^{-8.16}$ M) was much lower than that of sulfate ions ($\{SO_4^{2-}\} = 10^{-2.29}$ M). Therefore, gypsum formation (SI = −0.68) is favored over calcite (SI = −2.17) at cement surface Layer I. In the inner Layers II and III, solution pH in the inner pores would be much higher, reported as around 10–13 (Kutchko et al., 2007, Duguid and Scherer, 2010) under ambient conditions. Under GCS conditions, the diffusion of proton into inner layers might be limited, resulting in higher pH in inner pore solutions. At higher pH values, the activity of carbonate ions in the inner pore solutions ($\{CO_3^{2-}\} = 10^{-3.07}$ M at pH = 10.00) could be much higher than in the solution near cement surfaces ($\{CO_3^{2-}\} = 10^{-8.16}$ M at pH = 4.04), and the pore solutions were supersaturated with respect to calcite (SI = 2.81 at pH = 10). Therefore, calcite formation is favored over gypsum (SI = −0.79) in the inner layers of reacted cement samples.

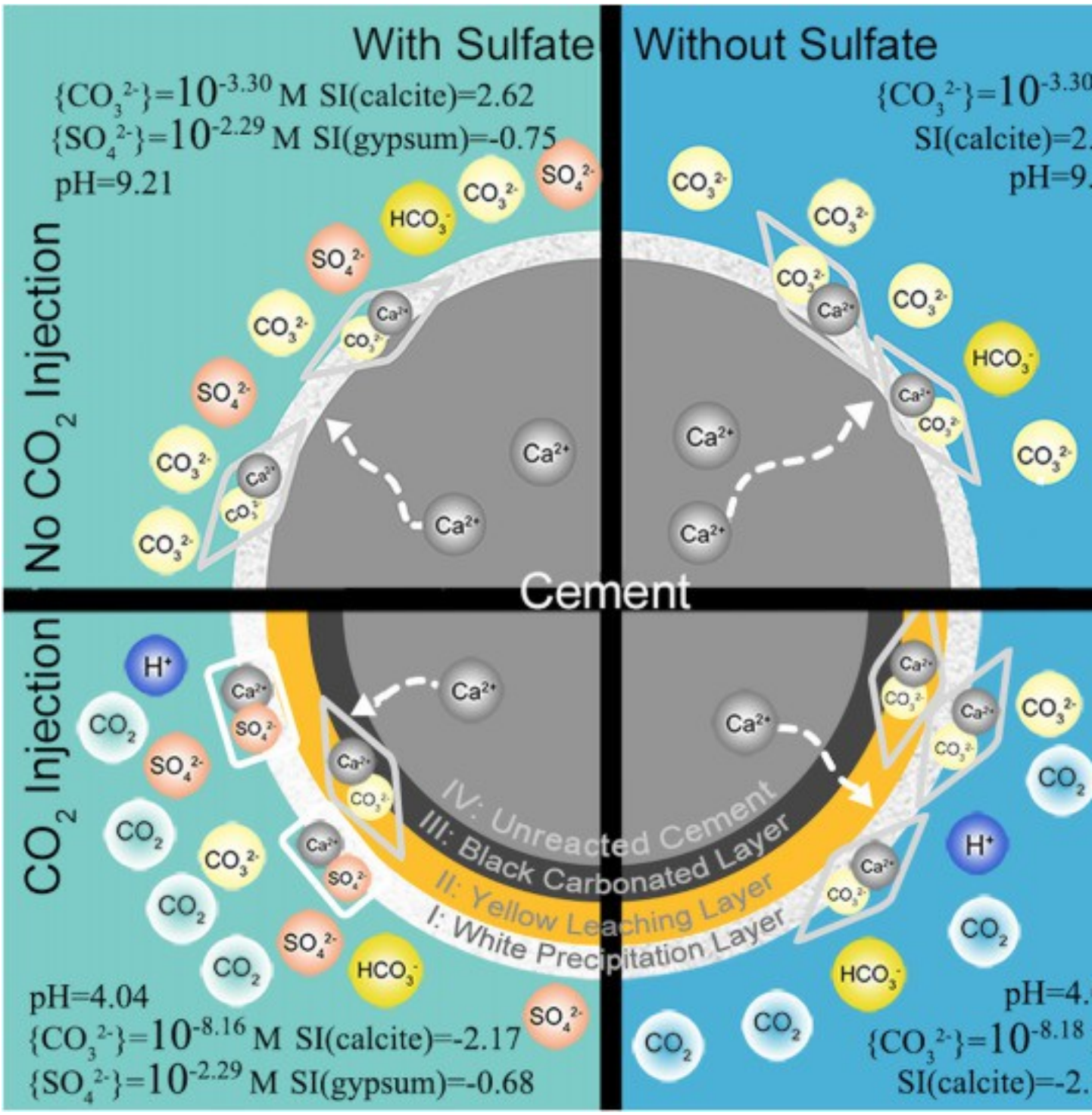

1. Download high-res image (971KB)
2. Download full-size image

Fig. 6. Schematic picture of the effects of CO_2 injection and sulfate ions on gypsum and calcite formation on cement surfaces and the inner layers. Top images: under 50 °C and 1 atm air in the presence (top left) and absence (top right) of sulfate,

calcite formed on cement surfaces in both solutions with high pH values. Bottom left image: under 50 °C and 100 atm in the presence of sulfate, gypsum formed in white precipitation layer I and calcite formed in the inner Layers II and III; Bottom right image: under 50 °C and 100 atm CO_2 in the absence of sulfate, calcite formed in both white precipitation Layer I and the inner Layers II and III. Activities for CO_3^{2-} ($\{CO_3^{2-}\}$) and SO_4^{2-} ($\{SO_4^{2-}\}$) in the bulk solution, and the bulk solutions' saturation indices (SI) with respect to calcite and gypsum were calculated by GWB.

If our hypothesis is correct, then for our control experiments conducted under atmospheric pressure conditions (1 atm air, 50 °C) in the presence of sulfate with a high bulk solution pH value ~9.21, the high activity of CO_3^{2-} ($\{CO_3^{2-}\} = 10^{-3.30}$ M) should result in calcite (SI = 2.62) formation on the cement surfaces rather than gypsum (SI = −0.75) (Fig. 6). Since the precipitation layer on the reacted cement surface was too thin to collect enough powder for XRD analysis, the particles formed in solution after cement degradation were analyzed by XRD. As shown in Fig. 7, calcite, aragonite, and halitewere detected by XRD while gypsum was not detected, which validated our hypothesis.

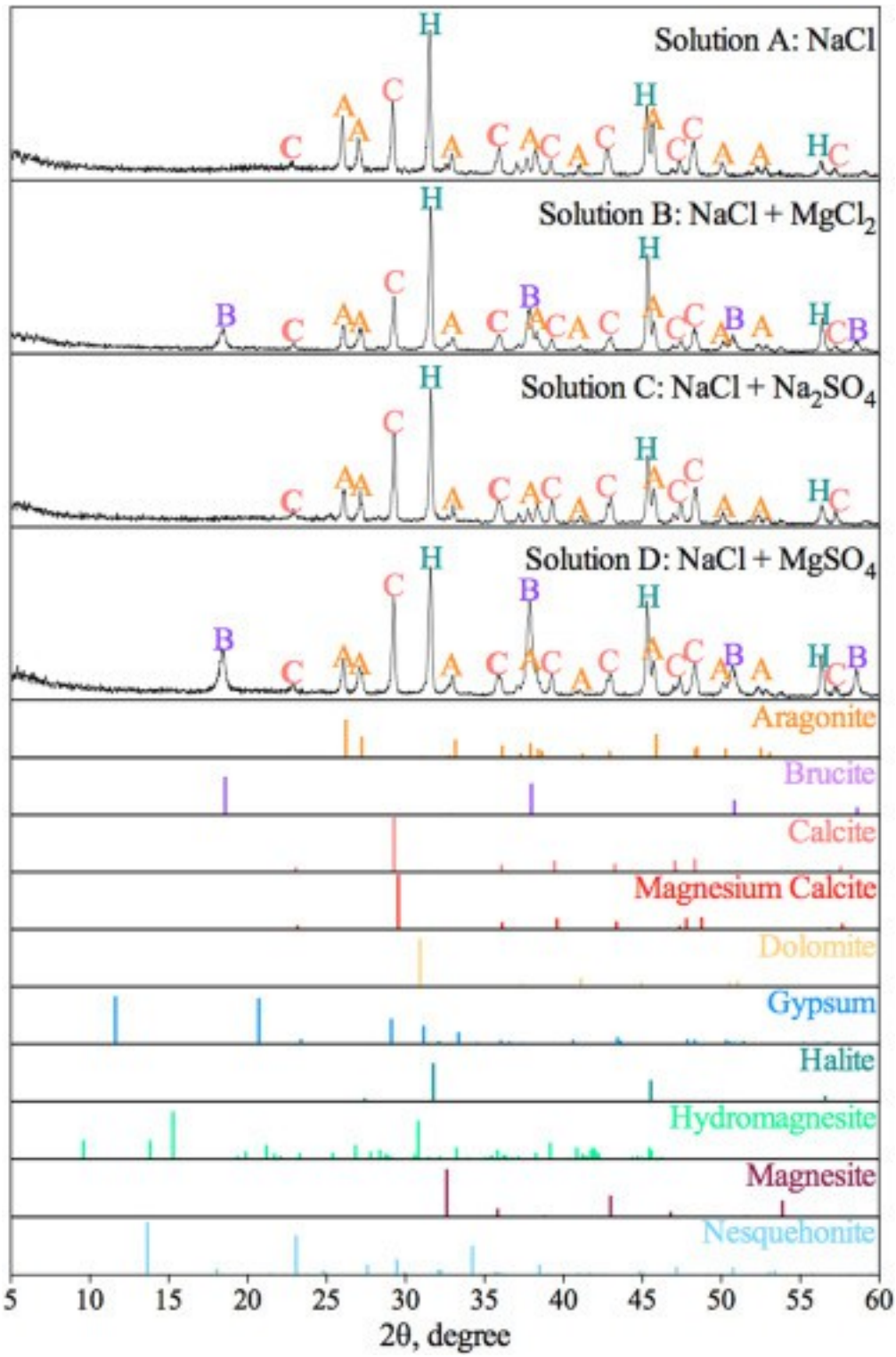

1. Download high-res image (514KB)
2. Download full-size image

Fig. 7. XRD analysis of precipitates in solution after cement degradation under atmospheric pressure (50 °C, 1 atm air) in synthetic brines (Table 1, solution A–D).

The effects of solution pH on gypsum and calcite formation during cement degradation have been reported previously under atmospheric conditions. Liu et al. (2015) investigated cement degradation at different pH values from 7 to 13 in sulfate solutions, and lower pH was found to favor gypsum formation. Bellmann et al. (2006) also investigated cement degradation and gypsum formation under variable pH conditions and found that at higher pH conditions, the minimum sulfate concentration needed for gypsum formation was higher. This is presumably due to the lower Ca concentrations in the pore space due to favored calcite precipitation under high pH conditions.

3.3. Slower cement degradation in the presence of sulfate

The depth of the carbonated layer has usually been used to evaluate cement degradation rate (Kutchko et al., 2007, Carey, 2013). Here the carbonation depths of cement samples reacted under 50 °C and 100 atm in different solutions (Table 1, solution A-D) were characterized by optical microscopy, and the carbonation front was identified as the interface between the black carbonated Layer III and the grey unreacted cement core (Fig. 1c). As shown in Fig. 8, in the presence of sulfate (solution C and D), the carbonation rates were slower than in the absence of sulfate (solution A and B). Similar trends were reported by Li et al. (2015b), where no gypsum was directly detected in their study, it was proposed that the coating of gypsum on calcite surface passivated the calcite crystals under acidic conditions (Huminicki and Rimstidt, 2008, Soler et al., 2008, Wilkins et al., 2001). In our study, based on XRD and SEM coupled with EDS/BSE, gypsum was detected for the first time on cement surfaces reacted under relevant GCS conditions in the presence of sulfate, while calcite formed in the absence of sulfate. Compared with calcite, the gypsum precipitates as coatings on cement might have prevented further brine and CO_2 attack on the cement, leading to the observed decreased cement degradation rates. In Li et al. (2015b)'sstudy, gypsum was not detected presumably due to the higher liquid to cement ratio (16:1) used there as compared with this study (10:1). The lower liquid-to-cement ratio used in this study may have resulted in a higher local Ca^{2+}concentration near cement surface, forming significant amounts of gypsum.

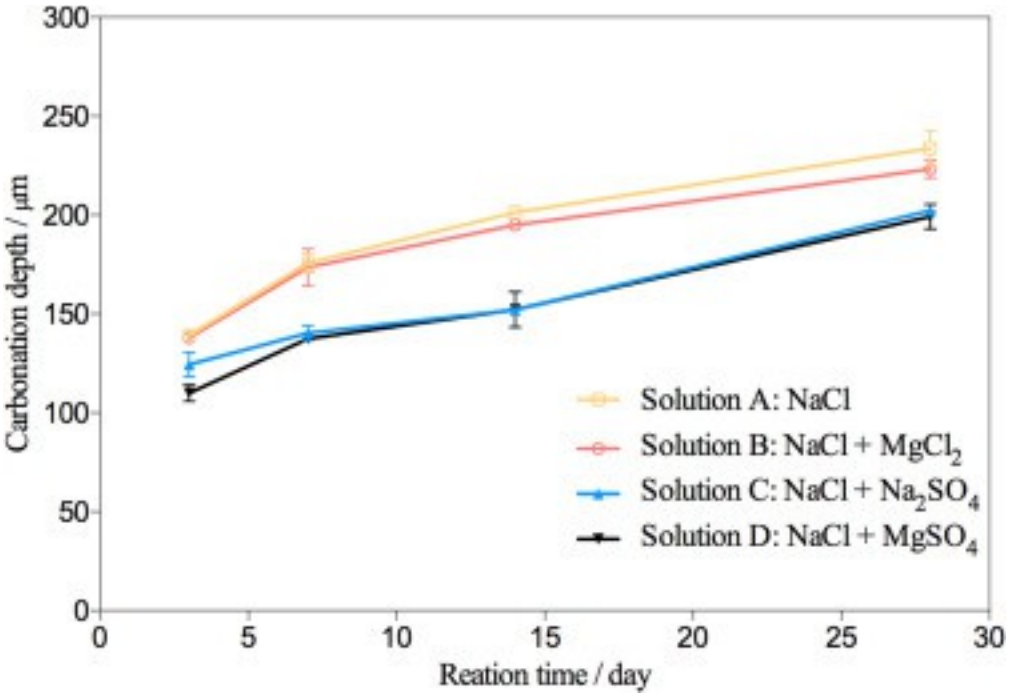

1. Download high-res image (221KB)
2. Download full-size image

Fig. 8. Carbonation depths of cement samples after different reaction periods (3, 7, 14, or 28 days) under GCS conditions (50 °C and 100 atm) in synthetic brines (Table 1, solution A–D).

3.4. Effects of Mg^{2+} on cement degradation under GCS conditions

Under ambient conditions, it was reported that cement attack by Mg^{2+} and SO_4^{2-} could result in brucite ($Mg(OH)_2$) and gypsum formation on cement surfaces (Bonen and Cohen, 1992). As $Mg(OH)_2$ has a much lower solubility than $Ca(OH)_2$, in Mg^{2+}-containing solutions at neutral or basic pH conditions, brucite precipitation can occur, thus lowering the solution pH. This could promote $Ca(OH)_2$ dissolution and gypsum precipitation in the presence of SO_4^{2-}(Rasheeduzzafar et al., 1994). In the present study, under ambient pressure conditions, brucite was detected as precipitates in the brines in the presence of Mg^{2+} (Fig. 7). In contrast, under relevant GCS condition, no brucite was detected in layers I–III by XRD analysis (Fig. 4, Fig. 5). Because under GCS conditions, the pH in the brine solution near cement surface was ~4, thus the solution was undersaturated with respect to brucite and magnesium carbonate minerals (GWB calculations in Table S1 in Supporting information). Thus, no brucite or magnesium carbonate minerals were detected in layer I (Fig. 4). In the inner layers II and III, as discussed earlier in Section 3.2, the pore solution had a much higher pH, due to the limited diffusion of proton into inner pores. If we assume Mg concentration in inner pores was the same as

in bulk solution, the pore solution would have been supersaturated with respect to brucite and magnesium carbonate minerals (GWB calculations in Table S1 in Supporting information). However, no brucite or magnesium carbonate was detected in inner layers II and III (Fig. 5), indicating limited diffusion of Mg ions into inner layer pores and much lower Mg concentrations in cement inner layers than in bulk solution.
The potential formation of magnesium calcite was also considered. With Mg incorporation, the XRD peaks of calcite can shift due to the reduction of unit cell dimensions (Falini et al., 1998, Kralj et al., 2004). According to MINCRYST (Chichagov, 1990), with 6 mol%, 10 mol% and 13 mol% of Mg incorporation, the strongest diffraction peak of calcite shifted from 29.27° to 29.554°, 29.733°, and 29.761°, respectively (Fig. S5 in Supporting information). Here the XRD peaks of calcite formed in the presence and absence of aqueous Mg showed no discernable differences (Fig. S5 in Supporting information), indicating little magnesium incorporation in calcite. A higher aqueous Mg/Ca ratio was reported to promote Mg incorporation into calcite (Kralj et al., 2004). At 25 °C, Mg was observed to incorporate into calcite with aqueous Mg/Ca ratios of 1:1 and 2:1, while no Mg incorporation was observed with a ratio of 0.5:1. In the present study, the Mg/Ca ratio in bulk solution was 5:1. However, the local Ca concentration in layers I–III could be much higher than in the bulk, considering the local Ca ion supply from leached layer II and the limited diffusion of Mg into inner layers. Therefore, the local aqueous Mg/Ca ratios in layers I–III could be much lower than in the bulk solution, resulting in little Mg incorporation during calcite precipitation. The absence of brucite, magnesium carbonate, and magnesium calcite formation could presumably explain why Mg^{2+} had no significant effect on cement degradation under GCS conditions (Fig. 8).

4. Conclusions and implications

The effects of sulfate and magnesium ions on CO_2-brine-cement interactions were investigated in this study under relevant GCS conditions, at 50 °C under 100 atm CO_2. SEM-EDS/BSE and XRD measurements showed that gypsumformed on the surface of the reacted cement samples in the presence of sulfate, due to the presence of high sulfate concentration, a low liquid-to-solid ratio and low solution pH resulting from CO_2 dissolution. In the inner layers of reacted cement samples where higher pH in the pore solution was expected, calcite instead of gypsum formed. For cement reacted under atmospheric pressure conditions with high solution pH, calcite rather than gypsum precipitated. Based on these observations, the effects of solution pH on carbonate ion activities were shown to control whether gypsum or calcite was the primary precipitate. Furthermore, the gypsum coatings on reacted cement was found to

prevent further CO_2 and brine attack on cement, resulting in a slower carbonation in the presence of sulfate. In contrast, magnesium did not show a significant effect on cement degradation under GCS conditions, as brucite, magnesium carbonates, and magnesium calcite did not form due to the low solution pH on cement surfaces and limited Mg ion diffusion into cement inner layers.

This study provided valuable insights into cement degradation under GCS conditions in brines with different compositions, which can be valuable for the site selectionsand GCS operations. Cement expansion and cracking by mineral formation requires mineral precipitation occurring inside cement (Santhanam et al., 2003). Based on current study conducted under GCS conditions, gypsum formed only on the surface of the reacted cement samples, instead of in the inner layers of cement, indicating that it may not cause cement expansion and cracking. Instead, the formation of gypsum on cement surface helped to prevent further CO_2 and brine attack, and resulted in slower cement degradation, which is quite different from sulfate attack under ambient conditions. However, experiments of longer time durations are needed to quantify the long-term reactions, which can be an important future direction.

Acknowledgments

This work was supported by the Center for Nanoscale Control of Geologic CO_2, an Energy Frontier Research Center funded by the U.S. Department of Energy, Office of Science, Basic Energy Sciences under Contract No. DE-AC02-05CH11231to Lawrence Berkeley National Laboratory. We also acknowledge the partial support by National Natural Science Foundation of China (41272061, 41472232) and Science and Technology Innovation Fund of the China University of Geosciences (Beijing).

Appendix A. Supplementary data

The following is Supplementary data to this article:

Download Word document (11MB)Help with docx files

References

API, 2005

R. API**10B-2. Recommended Practice for Testing Well Cements**

(2005)

Bellmann et al., 2006

F. Bellmann, B. Möser, J. Stark**Influence of sulfate solution concentration on the formation of gypsum in sulfate resistance test specimen**

Cem. Concr. Res., 36 (2006), pp. 358-363

ArticleDownload PDFView Record in Scopus

Bonen and Cohen, 1992

D. Bonen, M.D. Cohen**Magnesium sulfate attack on Portland cement paste—I. Microstructural analysis**

Cem. Concr. Res., 22 (1992), pp. 169-180

ArticleDownload PDFView Record in Scopus

Carey et al., 2007

J.W. Carey, M. Wigand, S.J. Chipera, G. WoldeGabriel, R. Pawar, P.C. Lichtner, S.C. Wehner, M. A. Raines, G.D. Guthrie Jr**Analysis and performance of oil well cement with 30 years of CO_2 exposure from the SACROC unit, West Texas, USA**

Int. J. Greenh. Gas Control, 1 (2007), pp. 75-85

ArticleDownload PDFView Record in Scopus

Carey, 2013

J.W. Carey**Geochemistry of wellbore integrity in CO_2 sequestration: Portland cement-steel-brine-CO_2 interactions**

Rev. Mineral. Geochem., 77 (2013), pp. 505-539

CrossRefView Record in Scopus

Chichagov, 1990

A.V. Chichagov**Information-calculating system on crystal structure data of minerals (MINCRYST)**

Kristallographiya, 35 (1990)

Crow et al., 2010

W. Crow, J.W. Carey, S. Gasda, D.B. Williams, M. Celia**Wellbore integrity analysis of a natural CO_2 producer**

Int. J. Greenh. Gas Control, 4 (2010), pp. 186-197

ArticleDownload PDFView Record in Scopus

Dai and Hu, 2015

C. Dai, Y.D. Hu**Fe(III) hydroxide nucleation and growth on quartz in the presence of Cu(II), Pb(II), and Cr(III): metal hydrolysis and adsorption**

Environ. Sci. Technol., 49 (3) (2015), pp. 292-300

CrossRefView Record in Scopus

Dai et al., 2016

C. Dai, X.B. Zuo, B. Cao, Y.D. Hu**Homogeneous and heterogeneous precipitation of $(Fe_x, Cr_{1-x})(OH)_3$ nanoparticles: implications for aqueous Cr removal**

Environ. Sci. Technol., 50 (4) (2016), pp. 1741-1749

CrossRefView Record in Scopus

De Silva et al., 2015

G.P.D. De Silva, P.G. Ranjith, M.S.A. Perera**Geochemical aspects of CO_2 sequestration in deep saline aquifers: a review**

Fuel, 155 (2015), pp. 128-143
ArticleDownload PDFView Record in Scopus

Duguid and Scherer, 2010

A. Duguid, G.W. Scherer**Degradation of oilwell cement due to exposure to carbonated brine**
Int. J. Greenh. Gas Control, 4 (2010), pp. 546-560
ArticleDownload PDFView Record in Scopus

Duguid, 2009

A. Duguid**An estimate of the time to degrade the cement sheath in a well exposed to carbonated brine**
Energy Procedia, 1 (2009), pp. 3181-3188
ArticleDownload PDFView Record in Scopus

Falini et al., 1998

G. Falini, S. Fermani, M. Gazzano, Ripamonti**Structure and morphology of synthetic magnesium calcite**
J. Mater. Chem., 8 (1998), pp. 1061-1065
CrossRefView Record in Scopus

Garcia-et-al.,-2012

D. Garcia, H.B. Shao, Y.D. Hu, J.R. Ray, Y.S. Jun**Supercritical CO_2-brine induced dissolution, swelling, and secondary mineral formation on phlogopite surfaces at 75–95 °C and 75 atm**
Environ. Sci. Technol., 5 (2) (2012), pp. 5758-5767
CrossRefView Record in Scopus

Hawthorne et al., 2011

S.B. Hawthorne, D.J. Miller, Y. Holubnyak, J.A.Harju, B.G. Kutchko, B.R. Strazisar**Experimental investigations of the effects of acid gas (H_2S/CO_2) exposure under geological sequestration conditions**
Energy Procedia, 4 (2011), pp. 5259-5266
ArticleDownload PDFView Record in Scopus

Hu and Jun, 2012

Y.D. Hu, Y.S. Jun**Biotite dissolution in brine at varied temperature and CO_2pressures: its activation energy and potential CO_2intercalation**
Langmuir, 28 (41) (2012), pp. 14633-14641
CrossRefView Record in Scopus

Hu et al., 2011

Y.D. Hu, J.R. Ray, Y.S. Jun**Biotite-brine interactions under acidic hydrothermal conditions: fibrous illite, goethite and kaolinite formation and biotite surface cracking**
Environ. Sci. Technol., 45 (14) (2011), pp. 6175-6180
CrossRefView Record in Scopus

Hu et al., 2013

Y.D. Hu, J.R. Ray, Y.S. Jun**Na^+, Ca^{2+}, and Mg^{2+} in brines affect supercritical CO_2–brine–biotite interactions: ion exchange, biotite dissolution, and illite precipitation**
Environ. Sci. Technol., 47 (1) (2013), pp. 191-197
ArticleDownload PDFCrossRefView Record in Scopus

Huminicki and R

D.M.C. Huminicki, J.D. Rimstidt**Neutralization of sulfuric acid solutions by calcite dissolution and the application to anoxic limestone drain design**
Appl. Geochem., 23 (2008), pp. 148-165
ArticleDownload PDFView Record in Scopus

IPCC, 2005

IPCC**IPCC Special Report on Carbon Dioxide Capture and Storage, Prepared by Working Group III of the Intergovernmental Panel on Climate Change**
Cambridge University Press (2005)

Jacquemet et al.

N. Jacquemet, J. Pironon, J. Saint-Marc**Mineralogical changes of a well cement in various H_2S-CO_2(-brine) fluids at high pressure and temperature**
Environ. Sci. Technol., 42 (2008), pp. 282-288
CrossRefView Record in Scopus

Jacquemet et al.

N. Jacquemet, J. Pironon, V. Lagneau, J. Saint-Marc**Armouring of well cement in H_2S-CO_2 saturated brine by calcite coating-experiments and numerical modelling**
Appl. Geochem., 27 (2012), pp. 782-795
ArticleDownload PDFView Record in Scopus

Keller, 1983

S.J. Keller**Analyses of Subsurface Brines of Indiana**
Department of Natural Resources, Bloomington, Ind (1983)

Kralj et al., 2004

D. Kralj, J. Kontrec, L. Brečević, G. Falini, V. Nöthig-Laslo**Effect of inorganic anions on the morphology and structure of magnesium calcite**
Chem. Eur. J., 10 (2004), pp. 1647-1656
CrossRefView Record in Scopus

Kutchko et al., 2

B.G. Kutchko, B.R. Strazisar, D.A. Dzombak, G.V.Lowry, N. Thaulow**Degradation of well cement by CO_2 under geologic sequestration conditions**
Environ. Sci. Technol., 41 (2007), pp. 4787-4792
CrossRefView Record in Scopus

Kutchko et al., 2

B.G. Kutchko, B.R. Strazisar, G.V. Lowry, D.A.Dzombak, N. Thaulow**Rate of CO_2 attack on hydrated Class H well cement under geologic sequestration conditions**
Envirnon. Sci. Technol., 42 (2008), pp. 6237-6242
CrossRefView Record in Scopus

Kutchko et al., 2

B.G. Kutchko, B.R. Strazisar, N. Huerta, G.V. Lowry, D.A. Dzombak, N. Thaulow**CO_2 reaction with hydrated Class H well cement under geologic sequestration conditions: effect of flyash admixtures**
Environ. Sci. Technol., 43 (2009), pp. 3947-3952
CrossRefView Record in Scopus

Kutchko et al., 2

B.G. Kutchko, B.R. Strazisar, S.B. Hawthorne, C.L.Lopano, D.J. Miller, J.A. Hakala, G.D. Guthrie **H_2S-CO_2 reaction with hydrated Class H well cement: acid-gas injection and CO_2 co-sequestration**
Int. J. Greenh. Gas Control, 5 (2011), pp. 880-888
ArticleDownload PDFView Record in Scopus

Li et al., 2015a

Q.Y. Li, Y.M. Lim, K.M. Flores, K. Kranjc, Y.S. Jun**Chemical reactions of Portland cement with aqueous CO_2 and their impacts on cement's mechanical properties under geologic CO_2 sequestration conditions**

Environ. Sci. Technol., 49 (2015), pp. 6335-6343

CrossRefView Record in Scopus

Li et al., 2015b

Q.Y. Li, Y.M. Lim, Y.S. Jun**Effects of sulfate during CO_2 attack on Portland cement and their impacts on mechanical properties under geologic CO_2sequestration conditions**

Environ. Sci. Technol., 49 (2015), pp. 7032-7041

CrossRefView Record in Scopus

Liu et al., 2015

K.W. Liu, L.W. Mo, M. Deng**Influence of pH on the formation of gypsum in cement materials during sulfate attack**

Adv. Cem. Res., 27 (2015), pp. 487-493

CrossRefView Record in Scopus

Neville, 2004

A. Neville**The confused world of sulfate attack on concrete**

Cem. Concr. Res., 34 (2004), pp. 1275-1296

ArticleDownload PDFView Record in Scopus

Pabalan et al., 2

R.T. Pabalan, F.P. Glasser, D.A. Pichett, G.R. Walter, S. Biswas, M.R. Juchett, L.M. Sabido, J.L. Myers**Review of Literature and Assessment of Factors Relevant to Performance of Grouted Systems for Radioactive Waste Disposal**

Center for Nuclear Waste Regulatory Analyses, San Antonio, Texas(2009)

Rasheeduzzafar

Rasheeduzzafar, O.S.B. Al-Amoudi, S.N.Abduljauwad, M. Maslehuddin**Magnesium-sodium sulfate attack in plain and blended cements**

J. Mater. Civ. Eng., 6 (1994), pp. 201-222

CrossRefView Record in Scopus

Santhanam et al

M. Santhanam, M.D. Cohen, J. Olek**Effects of gypsum formation on the performance of cement mortars during external sulfate attack**

Cem. Concr. Res., 33 (2003), pp. 325-332

ArticleDownload PDFView Record in Scopus

Scherer et al., 20

G.W. Scherer, B. Kutchko, N. Thaulow, A. Duguid, B.Mook**Characterization of cement from a well at teapot dome oil field: implications for geological sequestration**

Int. J. Greenh. Gas Control, 5 (2011), pp. 115-124

ArticleDownload PDFView Record in Scopus

Soler et al., 2008

J.M. Soler, M. Boi, J.L. Mogollón, J. Cama, C. Ayora, P.S. Nico, N. Tamura, M. Kunz**The passivation of calcite by acid mine water. Column experiments with ferric sulfate and ferric chloride solutions at pH 2**

Appl. Geochem., 23 (2008), pp. 3579-3588

ArticleDownload PDFView Record in Scopus

Tian and Cohen,

B. Tian, M.D. Cohen**Does gypsum formation during sulfate attack on concrete lead to expansion?**

Cem. Concr. Res., 30 (2000), pp. 117-123

ArticleDownload PDFView Record in Scopus

Tian and Cohen,

B. Tian, M.D. Cohen**Expansion of alite paste caused by gypsum formation during sulfate attack**

J. Mater. Civ. Eng., 12 (2000), pp. 24-25

CrossRefView Record in Scopus

Wilkins et al., 20

S.J. Wilkins, R.G. Compton, M.A. Taylor, H.A. Viles**Channel flow cell studies of the inhibiting action of gypsum on the dissolution kinetics of calcite: a laboratory approach with implications for field monitoring**

J. Colloid Interface Sci., 236 (2001), pp. 354-361

ArticleDownload PDFView Record in Scopus

Zhang and Bach

M. Zhang, S. Bachu**Review of integrity of existing wells in relation to CO_2geological storage: what do we know?**

Int. J. Greenh. Gas Control, 5 (2011), pp. 826-840

ArticleDownload PDFView Record in Scopus

Zhang et al., 201

L. Zhang, D.A. Dzombak, D.V. Nakles, S.B. Hawthorne, D.J. Miller, B.G. Kutchko, C.L. Lopano, B. R. Strazisar**Characterization of pozzolan-amended wellbore cement exposed to CO_2 and H_2S gas mixtures under geologic carbon storage conditions**

Int. J. Greenh. Gas Control, 19 (2013), pp. 358-368

ArticleDownload PDFView Record in Scopus

Zhang et al., 201

L.W. Zhang, D.A. Dzombak, D.V. Nakles, S.B.Hawthorne, D.J. Miller, B.G. Kutchko, C.L. Lopano, B.R. Strazisar**Rate of H_2S and CO_2 attack on pozzolan-amended Class H well cement under geologic sequestration conditions**

Int. J. Greenh. Gas Control, 27 (2014), pp. 299-308

$$CaCO_3 + H_2CO_3 \rightarrow Ca^{2+} + 2HCO_3^- \quad (1)$$

$$Ca^{2+} + OH^- + HCO_3^- \rightarrow CaCO_3 + H_2O \quad (2)$$